

Interaction Energy Analysis of Nonclassical Antifolates with *Pneumocystis carinii* Dihydrofolate Reductase

Conrad Pitts¹, Jian Yin¹, Donnell Bowen², Celia J. Maxwell³, and William M. Southerland^{1*}

¹Department of Biochemistry and Molecular Biology, Howard University College of Medicine, 520 “W” Street NW, Washington, D. C. 20059

²Department of Pharmacology, Howard University College of Medicine, 520 “W” Street NW, Washington, D. C. 20059

³Department of Medicine, Howard University College of Medicine, 2014 Georgia Ave. NW, Washington, D. C. 20059

*Author to whom correspondence should be addressed. E-mail: wsoutherland@howard.edu

Received: 7 June 2002 / Accepted: 30 October 2002 / Published: 30 November 2002

Abstract: The x-ray structure of the *Pneumocystis carinii* dihydrofolate reductase (DHFR):trimethoprim:NADPH ternary complex obtained from the Protein Databank was used as a structural template to generate models for the following complexes: *P. carinii* DHFR:piritrexim:NADPH, *P. carinii* DHFR:epiroprim:NADPH, and *P. carinii* DHFR:trimetrexate:NADPH. Each of these complexes, including the original trimethoprim complex was then modeled in 60 angstrom cubes of explicit water and minimized to a rms gradient between 1.0 to 3.0×10^{-5} kcal/angstrom. Subsequently, each antifolate structure was subdivided into distinct substructural regions. The minimized complexes were used to calculate interaction energies for each intact antifolate and its corresponding substructural regions with the *P. carinii* DHFR binding site residues, the DHFR protein, the solvated complex (which consists of *P. carinii* DHFR, NADPH, and solvent water), solvent water alone, and NADPH. Antifolate substructural regions which contained nitrogen and carbon atoms in an aromatic environment (i. e. the pteridyl, pyridopyrimidinyl, and diaminopyrimidinyl subregions) contributed most to the stability of antifolate interactions, while interaction energies for the hydrocarbon aromatic rings, methoxy, and ethoxy groups were much less stable. Additionally, interaction energy analyses were calculated for carbon and nitrogen atoms of the pteridyl, pyridopyrimidinyl, and diaminopyrimidinyl subregions and for the carbon and oxygen atoms of methoxy and ethoxy subregions. The contributions of hydrogen atoms were included with those of the carbon, nitrogen and oxygen atoms to which they are attached. These analyses revealed that the carbon atoms of the pteridyl,

pyridopyrimidinyl, and diaminopyrimidinyl subregions generally contributed most to the stability of those regions. Carbon atoms also contributed favorably to the stability of the methoxy group interactions. Those substructural regions which exhibit relatively unfavorable interaction energies may constitute important modification targets in the design of improved *P. carinii* DHFR inhibitors. Interaction energies for different groups of atoms within the substructural regions suggest strategies for modification of the substructural regions.

Keywords: antifolates, interaction energy, DHFR binding.

Introduction

Pneumocystis carinii pneumonia (PCP) is a common opportunistic infection in patients with AIDS [1-4]. An important therapeutic rationale for the treatment of PCP is the inhibition of dihydropteroate synthase (an enzyme of the folate synthesis pathway in microorganisms) and the inhibition of dihydrofolate reductase (DHFR). The principal treatment for PCP is the antifolate, trimethoprim (TMP) in combination with sulfamethoxazole, an inhibitor of dihydropteroate synthase [5]. Trimetrexate (TMQ) or piritrexim (PTX) may be used to treat patients who do not respond to or cannot tolerate the TMP:sulfamethoxazole combination [6,7,8]. Current treatment regimens for PCP are generally hampered by undesirable adverse reactions in some patients and by poor selectivity between the human and *P. carinii* DHFR molecules [9,10,11,12]. As a result, numerous investigations have focused on the development of improved and more selective inhibitors of *P. carinii* DHFR relative to the human DHFR [13,14,15,16].

It should be noted that antifolates are structurally complex molecules consisting of distinct substructural regions or modules and that the development of new antifolates often involves the structural modification of an existing antifolate structure. Consequently, modification of existing antifolate structures necessarily involves modification of one or more antifolate substructural regions. For example, Piper et. al. [13] synthesized analogs of trimetrexate (TMQ) and piritrexim (PTX) with modified phenyl groups. In general these analogs consisted of changes in the phenyl group substituents and their positions around the phenyl ring. They observed that phenyl groups with polar substituents resulted in improved antifolate binding. Those phenyl groups which contained a methoxy group and a methyltrifluoro group as substituents bound better to the *P. carinii* DHFR than analogs whose phenyl subregions contained less polar substituents. Additionally, TMQ analogs with carboxyl containing groups attached to the phenyl subregion also generally showed improved binding to *P. carinii* DHFR but not necessarily improved selectivity relative to the human DHFR [16]. When modification of the TMQ phenyl subregion did not increase the polarity of the phenyl subregion, binding to the *P. carinii* DHFR was not improved [13,16]. Moreover, if the binding of each

substructural region could be evaluated independently, those substructural regions which contribute less to overall binding could then be targeted for structural modification in order to enhance antifolate binding.

We report here interaction energy calculations for the interaction of PTX, TMQ, TMP, and epiroprim (EPM) and their respective substructural regions with the *P. carinii* DHFR binding site residues, the DHFR protein, the solvated complex (*P. carinii* DHFR, NADPH, and solvent water), solvent water alone, and NADPH. These results clearly provide new insight into improved design strategies in the development of new antifolate structures.

Materials and Methods

The x-ray structure of the *P. carinii* DHFR:TMP:NADPH complex [17] was obtained from the Protein Databank. Using the molecular editor facility of QUANTA, the molecular modeling software from Accelrys Inc, the TMP component of this complex was sequentially converted to EPM, PTX, and TMQ, resulting in the molecular models for the *P. carinii* DHFR:EPM:NADPH, *P. carinii* DHFR:TMP:NADPH, and *P. carinii* DHFR:TMQ:NADPH complexes. These complexes and the original *P. carinii* DHFR:TMP:NADPH complex were then modeled inside 60-angstrom cubes of explicit water. Water molecules were generated based on the TIP3P model [18]. The density of water in the cube was approximately 1.0 gram/milliliter. Each solvated complex was minimized to a rms gradient of 1.0 to 3.0×10^{-5} kcal/angstrom using the Adopted-Basis Newton Raphson algorithm in CHARMM [19]. The DHFR binding site residues for each complex were defined as those DHFR residues which contained at least one atom that was 3.7 angstroms or closer to an antifolate atom. Distances between antifolate atoms and DHFR atoms were calculated using the COOR DIST function in CHARMM. CHARMM was used to calculate the Van der Waals and electrostatic components of the interaction energies. Interaction energies values reported here represent the sum of these components. Interaction energies were calculated for each intact antifolate and each of its corresponding substructural regions with the *P. carinii* DHFR binding site residues (binding site); the *P. carinii* DHFR protein (DHFR); the hydrated complex (complex) which included *P. carinii* DHFR, NADPH, and solvent water; solvent water alone (water); and NADPH. Minimizations and interaction energy calculations were performed using a Silicon Graphics dual processor Octane workstation or a four processor Silicon Graphics origin200 server.

Results

The antifolate molecular structure may be considered to consist of separate modules or substructural regions which contribute to overall antifolate binding (Figure 1). Interaction energy patterns for PTX and its substructural regions are shown in Figure 2. Both PTX and its pteridyl substructural region showed very similar interaction energy patterns (Figure 2). Their interaction with complex showed the

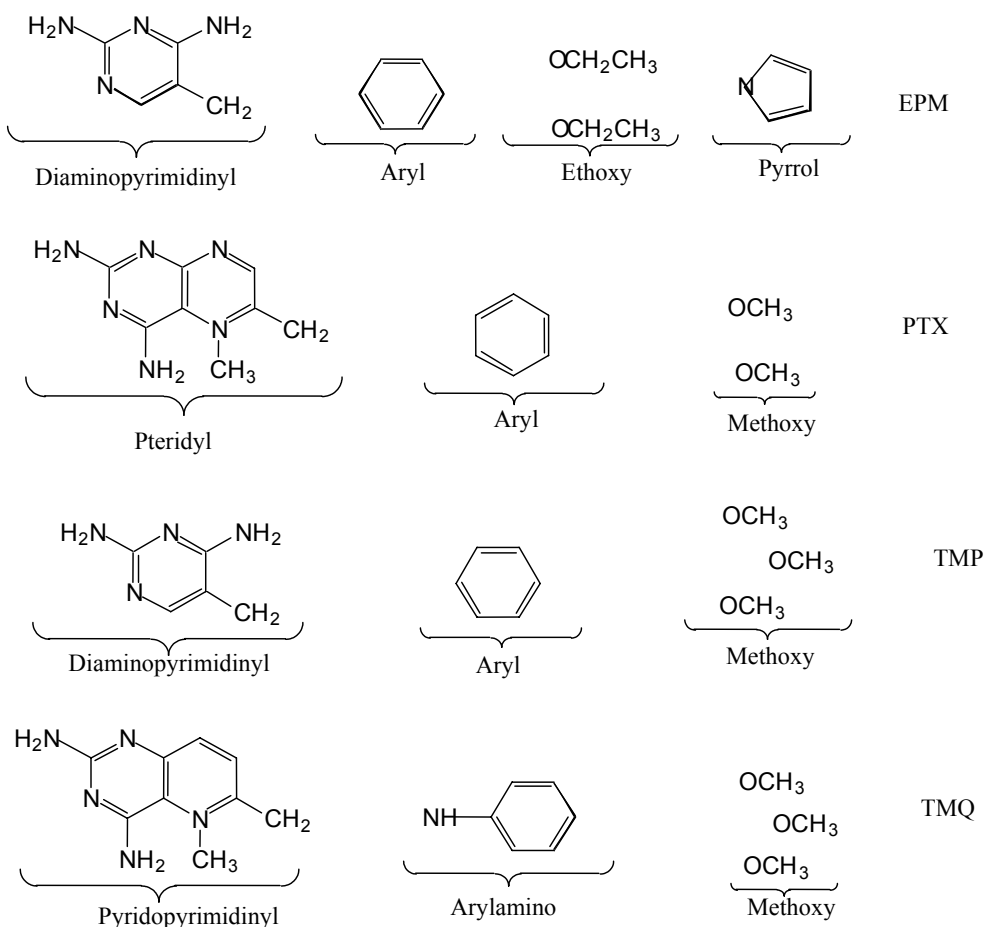


Figure 1. Substructural regions of EPM, PTX, TMP, and TMQ.

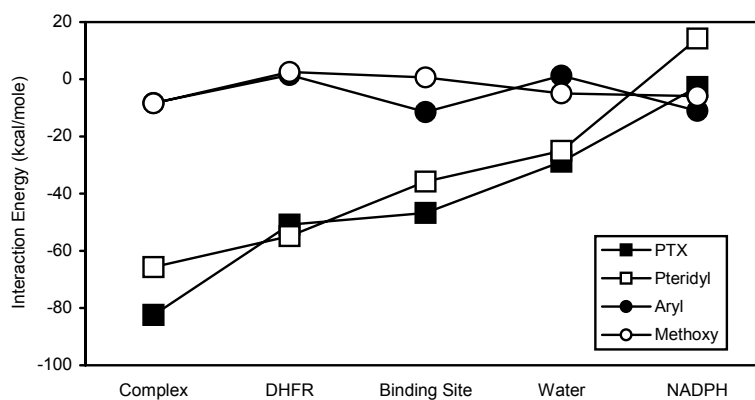


Figure 2. Comparison of interaction energy analyses of PTX and its substructural regions.

greatest stability followed by the interactions with DHFR, binding site, water, and NADPH, respectively. The pteridyl subregion was the major stabilizing contributor to the PTX interactions. The aryl and methoxy substructural regions contributed much less to the stability of the PTX interactions.

It was of interest to calculate the contribution of the pteridyl carbon and nitrogen atoms to the stability of the pteridyl interaction energies. These results are shown in Figure 3. The carbon atoms showed more stable interactions with binding site and NADPH, while the nitrogen atoms showed more stable interactions with complex, DHFR, and water. The carbon and oxygen atoms of the methoxy groups also made significantly different contributions to PTX binding (Figure 4). The methoxy carbon atoms showed more stable interactions with binding site and NADPH while the methoxy oxygen atoms showed more stable interactions with DHFR and water. Figure 4 revealed that the carbon atoms of the pteridyl and methoxy subregions of PTX interact favorably with binding site and NADPH and the nitrogen atoms of the pteridyl subregion and the oxygen atoms of the methoxy groups interact favorably with polar amino acid side chains of DHFR and solvent water.

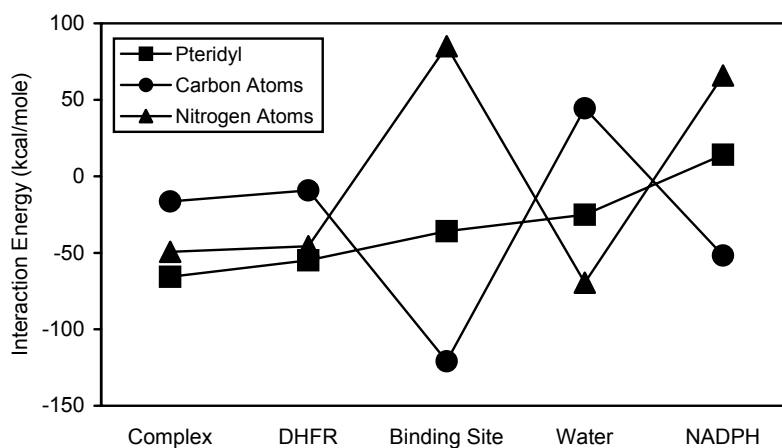


Figure 3. Comparison of interaction energy analyses of the pteridyl region of PTX with its carbon and nitrogen atoms.

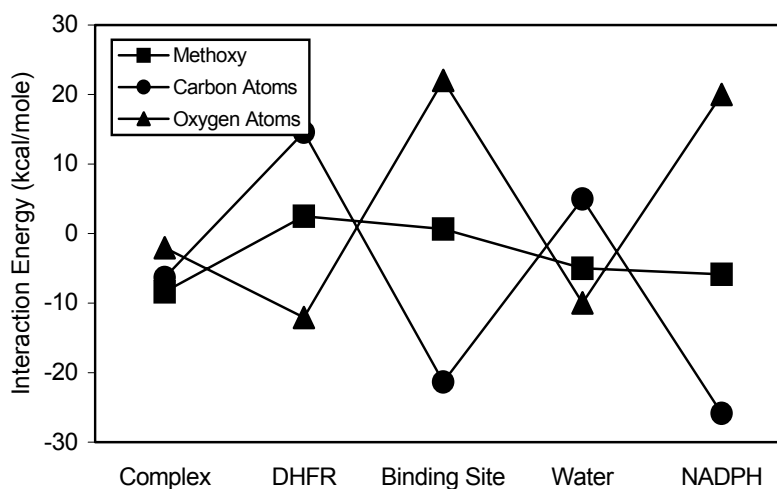


Figure 4. Comparison of the interaction energy analyses of the methoxy region of PTX and its carbon and oxygen atoms.

The diaminopyrimidinyl subregion of TMP was the major contributor to the stability of the TMP interactions (Figure 5). Both TMP and its diaminopyrimidinyl substructural region showed very similar interaction energy patterns. However, the TMP interactions were generally more stable than those of its diaminopyrimidinyl group. The diaminopyrimidinyl carbon atoms are clearly the major contributors to the stability of the diaminopyrimidinyl interactions (Figure 6). They showed favorable interactions with complex, binding site, and NADPH. The nitrogen atom interactions were much less stable. In fact, the most stable nitrogen atom interactions (DHFR and water) correspond to the least stable carbon atom interactions. Additionally, the carbon and nitrogen atoms of the diaminopyrimidinyl subregion showed opposing interaction energy patterns. The methoxy carbon and oxygen atoms exhibited opposing interaction energy patterns (Figure 7) with the oxygen atoms interacting favorably with DHFR and the carbon atoms interacting favorably with binding site and NADPH.

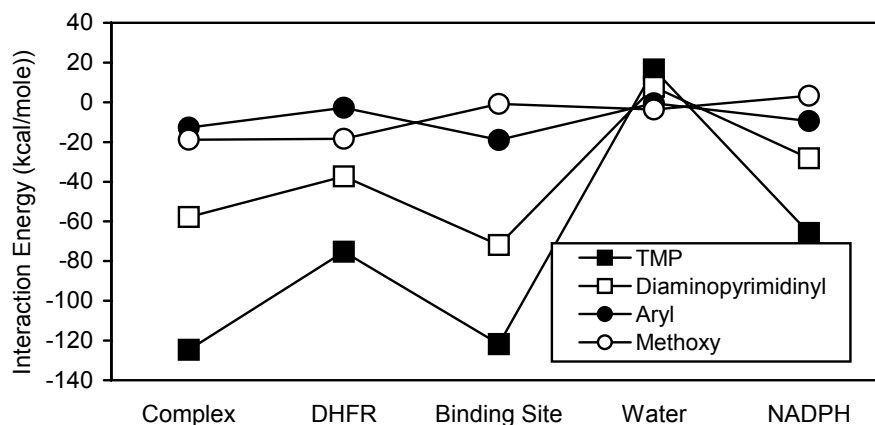


Figure 5. Comparison interaction energy analysis of TMP and its substructural regions.

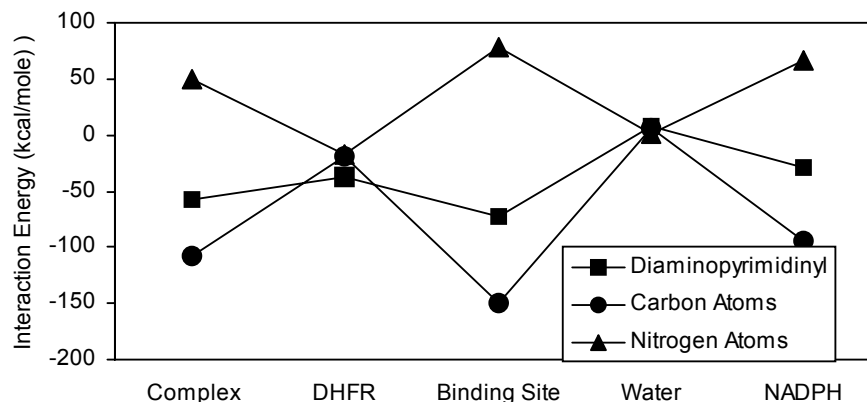


Figure 6. Comparison of interaction energy analysis of the diaminopyrimidinyl region of TMP with its carbon and nitrogen atoms.

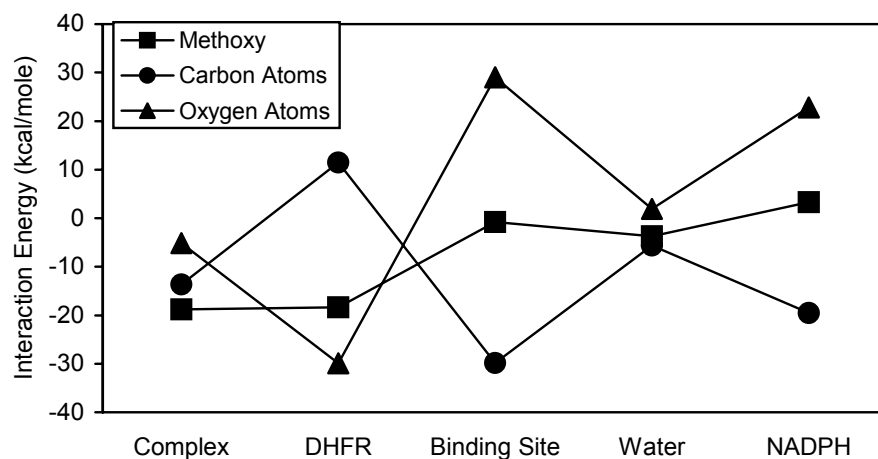


Figure 7. Comparison of interaction energy analysis of the methoxy region of TMP with its carbon and oxygen atoms.

The pyridopyrimidinyl substructural region is the primary contributor to the stability of the TMQ interactions (Figure 8). The carbon and nitrogen atoms of the pyridopyrimidinyl region also clearly exhibited opposing interaction energy patterns (Figure 9). The carbon atoms are the primary contributors to the stability of the pyridopyrimidinyl interactions. Their contributions to the complex interaction stability occurs primarily via the binding site and DHFR interactions. The arylamino subregion of TMQ consists of aromatic carbons and a non-aromatic nitrogen atom (Figure 1). The arylamino subregion and its carbon atoms exhibited almost identical interaction energy patterns. The arylamino nitrogen exhibited an interaction energy pattern and interaction energy values that were significantly different from those for the arylamino subregion and its carbon atoms (Figure 10). The methoxy carbon and oxygen atoms of TMQ generally showed opposing interaction energy patterns (Figure 11). The oxygen atoms showed more stable interactions with DHFR and water, while the carbon atoms showed more stable interactions with complex, binding site, and NADPH. The interaction energy analyses of EPM and its substructural regions are shown in Figure 12.

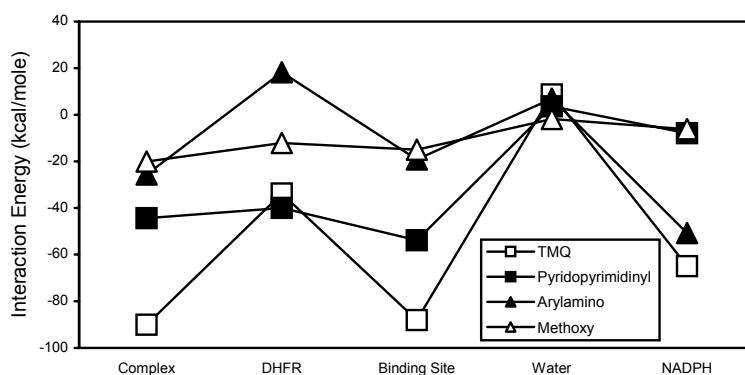


Figure 8. Comparison of interaction energy analysis TMQ and its substructural regions.

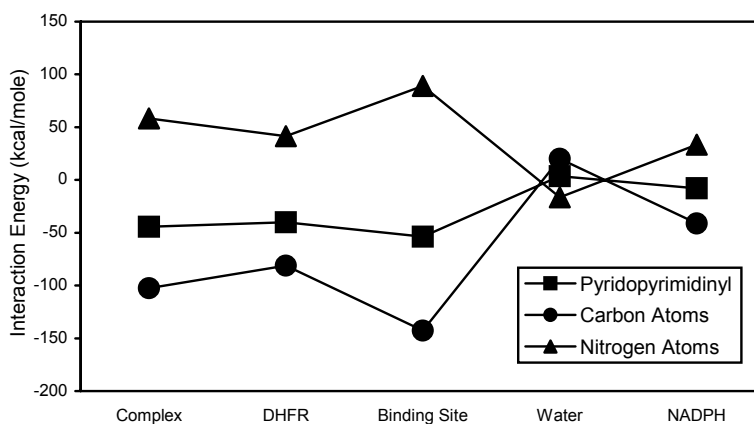


Figure 9. Comparison of interaction energy analysis of the pyridopyrimidinyl region of TMQ with its carbon and nitrogen atoms.

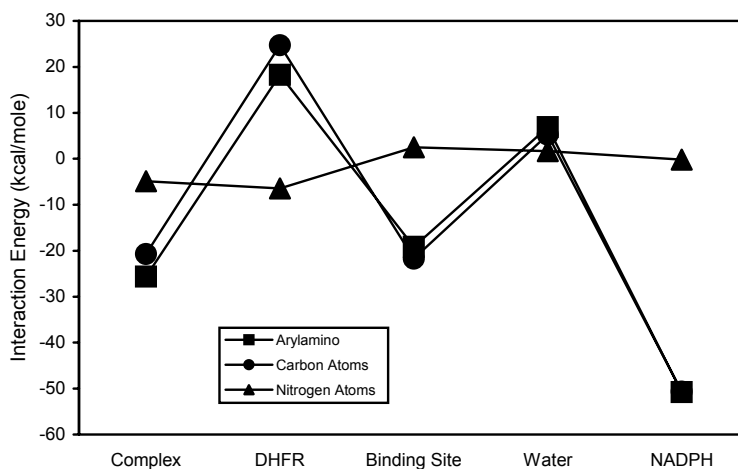


Figure 10. Comparison of interaction energy analysis of the arylamino region of TMQ with its carbon and nitrogen atoms.

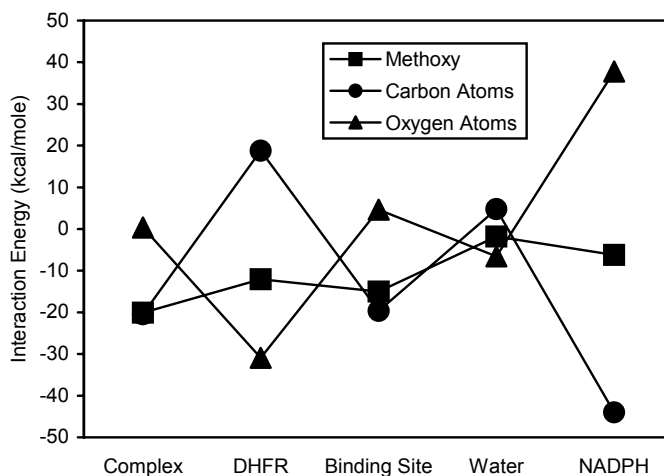


Figure 11. Comparison of interaction energy analysis of the methoxy regions of TMQ with its carbon and oxygen atoms.

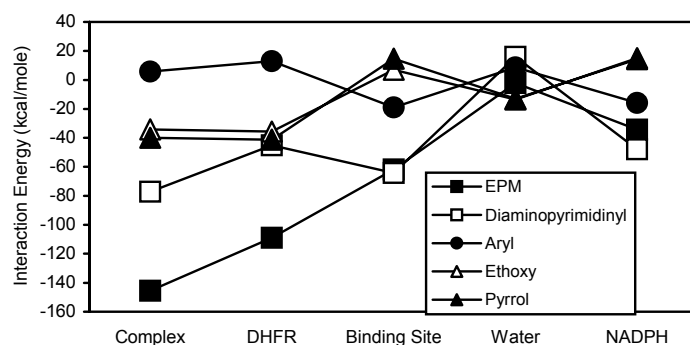


Figure 12. Comparison of interaction energy analysis of EPM and its substructural regions.

The EPM interactions with DHFR and binding site are the major contributors to the stability of the EPM interaction with complex. EPM and its diaminopyrimidinyl and aryl substructural regions showed similar interaction energy patterns for binding site, water, and NADPH. The contribution of each EPM substructural region to the interaction of intact EPM with complex may best be evaluated by considering the interactions of the individual subregions with complex. The Diaminopyrimidinyl subregion contributes most to the stability of the EPM interaction with complex while, the aryl group contributes least. The contributions of the ethoxy and pyrrol groups are intermediate between those of the aryl and diaminopyrimidinyl groups. The Diaminopyrimidinyl and aryl groups are hydrocarbon aromatic ring systems. However, the diaminopyrimidinyl group also contains two aromatic nitrogen atoms (Figure 1). The nitrogen and carbon atoms of the diaminopyrimidinyl group showed opposing interaction energy patterns (Figure 13). The carbon atoms showed more stable interactions with complex, binding site, and NADPH, while the nitrogen atoms showed more stable interactions with DHFR and water. The interaction of the carbon atoms with binding site is the primary stabilizing factor of the diaminopyrimidinyl interaction. The ethoxy oxygen and carbon atoms showed very similar interaction energy patterns, except for the complex and NADPH interactions (Figure 14).

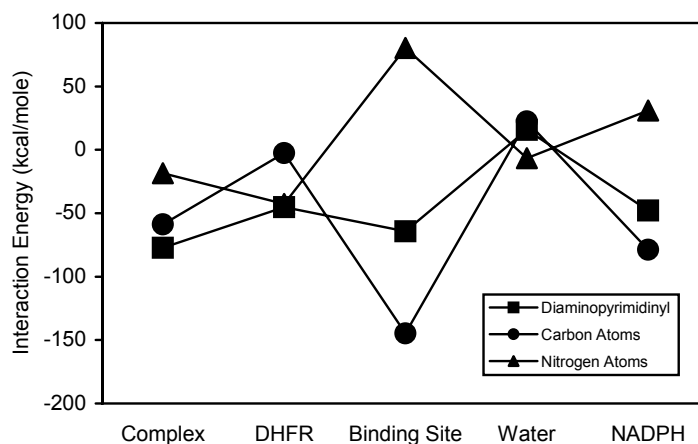


Figure 13. Comparison of interaction energy analysis of the diaminopyrimidinyl region of EPM with its carbon and nitrogen atoms.

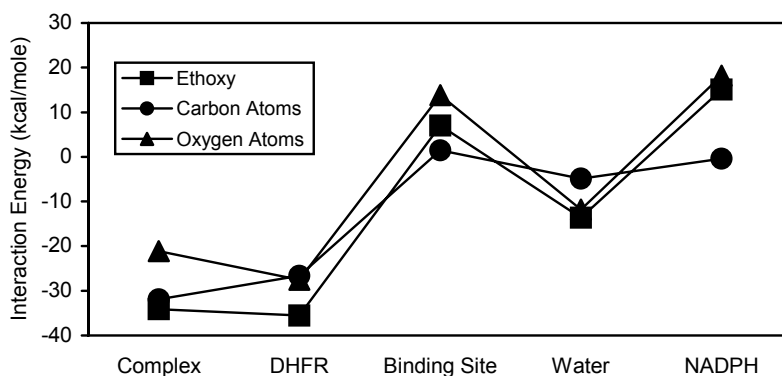


Figure 14. Comparison of interaction energy analysis of the ethoxy region of EPM with its carbon and oxygen atoms.

Table 1 shows the binding site residues for each of the bound antifolates. While each antifolate exhibit a different set of binding site residues, each binding site is characterized by a common subset of residues. The residues common to each antifolate binding site are ILE10, VAL11, ALA12, LEU25, GLU32, and ILE33. This subset of binding site residues may represent a more specific target in the design of new nonclassical antifolates for the inhibition of *P. carinii* DHFR.

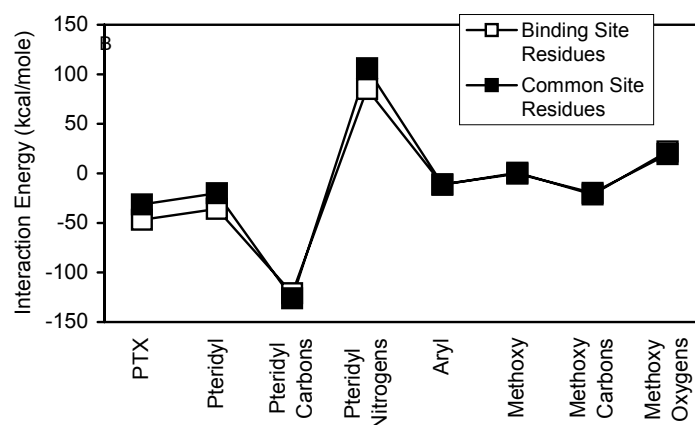
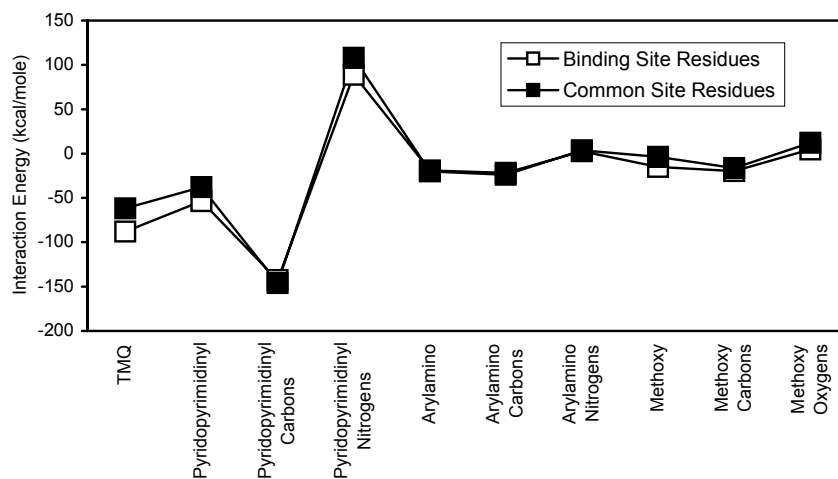
For each antifolate, the subset of common residues (common site residues) account for a significant portion of the corresponding binding site interactions (Table 2). In the cases of TMP and TMQ, the common site residues account for 77.4% and 70.30% of binding site interactions, respectively. These results clearly indicate that the common site residues are very important contributors to the stability of antifolate/binding site interactions. Additionally, figures 15, 16, 17 and 18 show that each antifolate and its substructural regions interact similarly with both binding site and common site residues.

Table 1. Comparison of Binding Site Residues for Each Antifolate/DHFR Complex

DHFR Complex	Binding Site Residues					
TMP	ILE10	VAL11	ALA12	LEU25	GLU32	ILE3
	PHE 36	SER64	PRO66	ILE123	TYR129	
PTX	ILE10	VAL11	ALA12	LEU25	GLU32	ILE33
	PHE36	PHE69	MET142	THR144		
TMX	ILE10	VAL11	ALA12	LEU25	GLU32	ILE33
	TYR35	THR61	SER64	ILE65	PRO66	MET142
	THR144					
EPM	ILE10	VAL11	ALA12	LEU25	GLU32	ILE33
	PHE36	PRO66	PHE69	ILE123	TYR129	

Table 2. Comparison of Antifolate Interaction Energies for *P. carinii* DHFR Binding Site and Common Binding Site Residues

Complex	Interaction Energies (kcal/mole)		
	Binding Site Residues	Common Site Residues	Common Site Residues x 100 / Binding Site Residues
TMP	-121.80	-94.27	77.40
PTX	-46.70	-31.28	66.98
EPM	-61.79	-27.47	44.45
TMQ	-88.05	-61.88	70.30

**Figure 15.** Comparison of binding site and common site interaction with PTX and its substructural regions.**Figure 16.** Comparison of binding site and common site interaction with TMQ and its substructural regions.

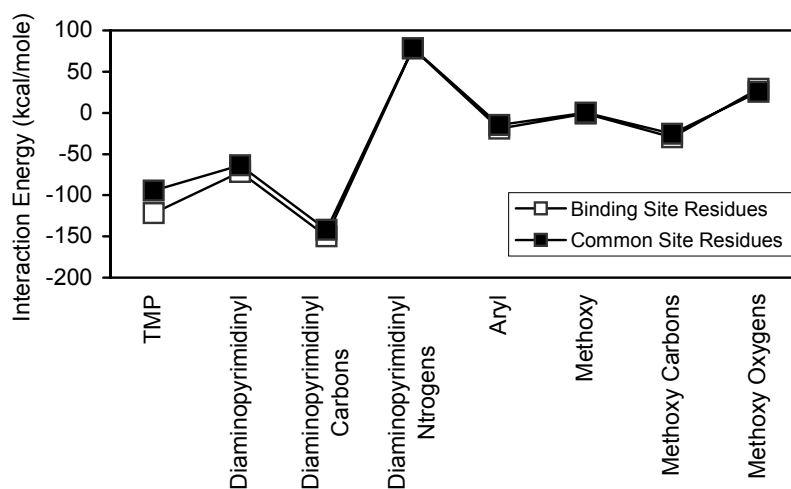


Figure 17. Comparison of binding site and common site interaction with TMP and its substructural regions.

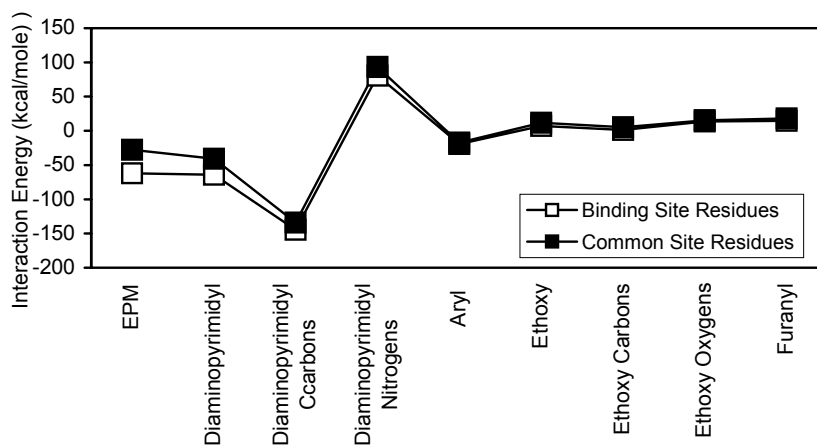


Figure 18. Comparison of binding site and common site interaction with EPM and its substructural regions.

Discussion

The pteridyl and pyridopyrimidinyl groups of PTX and TMQ, respectively and the diaminopyrimidinyl groups of TMP and EPM are the major contributors to the stability of their respective antifolate interactions with the solvated *P. carinii* DHFR complex. The carbon atoms of each of these subregions consequently showed favorable interactions with binding site and NADPH and the nitrogen atoms of these subregions showed unfavorable interactions with binding site and NADPH. Additionally, the carbon atoms generally showed unfavorable interactions with water and the nitrogen atoms generally showed stable interactions with water. Since the binding site of the *P. carinii* DHFR is a hydrophobic environment (Table 1), these observations indicate that the aromatic carbon atoms make favorable interactions with hydrophobic amino acid side chains of the *P. carinii* DHFR binding site and hydrophobic regions of NADPH, while the nitrogen atoms of these subregions

make relatively favorable interactions with water solvent molecules. These results also suggest that the pteridyl and pyridopyrimidinyl regions of PTX and TMQ and the diaminopyrimidinyl subregions of TMP and EPM are anchored to the *P. carinii* DHFR complex via both hydrophobic and hydrophilic interactions.

The solvated *P. carinii* DHFR complex may be viewed as one consisting of internal components (binding site, NADPH, and non-solvent exposed DHFR residues), and external components (solvent water, and solvent exposed DHFR residues). As a result, interaction energy patterns suggest that hydrophobic and hydrophilic interactions occur with internal and external components of the complexes, respectively. It is suggested that the favorable interaction energies exhibited by these subregions is due to their ability to employ both stable hydrophobic and stable hydrophilic interactions with internal and external components of the solvated complex. The ability to make stable interactions with both internal and external components of the complex may be an important factor in stable ligand binding.

The arylamino group TMQ, the aryl groups of EPM, PTX, and TMP are hydrocarbon aromatic rings. These groups generally exhibit significantly less favorable interaction energies with all components of the hydrated complex.

The methoxy groups of PTX, TMP, and TMQ exhibit similar interaction energy patterns as those observed for the hydrocarbon aromatic groups. However, the methoxy carbon atoms interact favorably with the hydrophobic environment of the binding site and presumably with hydrophobic components of the bound NADPH (internal components of the hydrated complex) while the methoxy oxygen atoms interact favorably with water and presumably polar side chains of DHFR (external components of the hydrated complex).

It is suggested that the development of new agents for the inhibition of *P. carinii* DHFR should include strategies for the design of antifolate structures with multiple subregions which have very favorable hydrophobic and hydrophilic interactions with internal and external components of the hydrated *P. carinii* DHFR complex.

Additionally, the presence of an apparent nonclassical antifolate binding core within the *P. carinii* DHFR binding site (an internal component of the complex) suggests that the core residues may play an important role in defining the contribution of binding site residues in the design of new agents for the inhibition of *P. carinii* DHFR.

Acknowledgements

This work was supported by grants RCMI-NIH 5G12RR03048 and NIGMS-NIH SO6GM0801628.

References

1. Mills, J. and Masur, H. AIDS-Related Infections. *Sci. Am.* **1991**, August, 50-57.
2. Gazard, B. G., Pneumocystis carinii pneumonia and its treatment in patients with AIDS. *J. Antimicrob. Chemother.* **1989**, 23 (suppl A), 67-75.
3. H., Problems in the management of opportunistic infections in patients infected with human immunodeficiency virus, *J. Infect. Dis.* **1990**, 161, 858-864.
4. Davey, R. T., Jr. and Masur, H., Recent advances in the diagnosis, treatment, and prevention of Pneumocystis carinii pneumonia, *Antimicrob. Agents Chemother.* **1990**, 34, 499-504.
5. Kovacs, J. A., Allegra, C. J., Swan, J. C., Drake, J. C., Parrillo, J. E., Chabner, B. A., and Masur, H., Potent antipneumocystis and antitoxoplasma activities of piritrexim, a lipid soluble antifolate, *Antimicrob. Agents Chemother.* **1988**, 32, 430-433.
6. Woods, D. D., The biochemical mode of action of the sulphonamide drugs, *J. Gen. Microbiol.* **1962**, 29, 687-702.
7. News. FDA Approves Trimetrexate As A Second line Therapy For Pneumocystis carinii Pneumonia, *Am J. Hosp. Pharm.* **1994**, 51, 591-592.
8. Allegra, C. J., chabner, B. A., Tuazon, C. U., Ogata-Arakaki, D., Baird, B., Drake, J. C., Simmons, T., Lack, E. E., Shelhamer, J. H., Balis, F., Walker, R., Kovacs, J. A., Lane, H. C., and Masur, H., Trimettexate for the treatment of Pnuemocystis carinii pneumonia in patients with the acquired immunodeficiency syndrome, *N. Engl. J. Med.* **1987**, 165, 926-931.
9. Gordin, F. M., Simon, G. L., Wofsy, C. B., and Mills, J., Adverse reactions to trimethoprim-sufamethoxazole in patients with acquired immunodeficiency syndrome, *Ann. Intern. Med.* **1984**, 100, 495-499.
10. Sattler, F. R., Cowan, R., Nielson, D. M., and Ruskin, J., Trimethoprim-sulfamethoxazole compared with pentamidine for treatment of pneumocystis carinii pneumonia in the acquired immunodeficiency syndrome, *Ann. Intern. Med.* **1988**, 109, 280-287.
11. Small, C. B., Harris, C. A., Friedland, G. H., and Klein, R. S., The treatment of Pneumocystis carinii pneumonia in the acquired immunodeficiency syndrome, *Arch. Intern. Med.* **1985**, 145, 837-840.
12. Sattler, F. R., Allegra, C. J., Verdegem, B., Akil, C. U. Tuazon, C. Hughlett, D., Ogata-Arakaki, J. Feinberg, J., Shelhamer, Lane, H. C., Davis, R., Boylen, C. T., Leedom, J. M., and Masur, H., Trimetrexate-leucovorin dosage evaluation study for treatment of Pneumocystis carinii pneumonia, *J. Infect. Dis.* **1990**, 161, 91-96.
13. Piper, J. R., Johnson, C. A., Krauth, C. A., Cater, R. L., Hosmer, C. A., Queener, S. F., Borotz, S. E., and Pfeifferkorn, E. R., Lipophilic Antifolates as Agents against Opportunistic Infections. I. Agents Superior to Trimetrexate and piritrexim against Toxoplasma gondii and pneumocystis carinii in in vitro Evaluations, *Antimicrob. Agents and Chemother.* **1996**, 40,1271-1280.
14. Jackson, H. C., Biggadike, K., McKilligin, E., Kinsman, O. S., Queener, S. F., Lane, A., and Smith, J. E., 6,7-Disubstituted 2,4 Diaminopteridines: Novel Inhibitors of Pneumocystis carinii and Toxoplasma gondii, *Antimicrob. Agents and Chemother.* **1996**, 40,1371-1375.

15. Rosowsky, A., Mota, C. E., Wright, J. E., and Queener, S. F., 2,4-Diamino-5-chloroquinazoline Analogues of Trimetrexate and Piritrexim: Synthesis and Antifolate Activity, *J. Med. Chem.* **1994**, *37*, 4522-4528.
16. Broughton, M. C. And Queener, S. F., Pneumocystis carinii Dihydrofolate Reductase Used to Screen Potential Antipneumocystis Drugs, *Antimicrob. Agents and Chemother.* **1991**, *35*, 1348-1355.
17. Champness, J. N., Achari, A., Ballantine, S. P., Bryant, P. K., Delves, C. J., and Stammers, D. K., The Structure of Pneumocystis carinii Dihydrofolate Reductase to 1.9 Angstroms Resolution, *Structure* **1994**, *2*, 915-924.
18. Jorgensen, W. L.; Chandrasekhar, J; Madura ,J. D.; Impey, R. W.; Klein, M. C., Comparison of Simple Potential Functions for Simulating Water, *J. Chem. Phys.* **1983**, *79*, 926-935.
19. Brooks, B. R.; Bruccoleri, R. E.; Olafson, B. D.; States, D. J.; Swaminathan, S.; Karplus, M., CHARMM: A Program for Macromolecular Energy Minimization, and Dynamics Calculations, *J. Comput. Chem.* **1983**, *4*, 187-217.